



**HAL**  
open science

# Development of a Robotic Ultrasound System to Assist Ultrasound Examination of Pregnant Women

Maria Bamaarouf, Flavien Paccot, Laurent Sarry, H el ene Chanal

► **To cite this version:**

Maria Bamaarouf, Flavien Paccot, Laurent Sarry, H el ene Chanal. Development of a Robotic Ultrasound System to Assist Ultrasound Examination of Pregnant Women. *IEEE Transactions on Medical Robotics and Bionics*, In press, 10.1109/TMRB.2024.3387047 . hal-04546186

**HAL Id: hal-04546186**

**<https://hal.science/hal-04546186v1>**

Submitted on 15 Apr 2024

**HAL** is a multi-disciplinary open access archive for the deposit and dissemination of scientific research documents, whether they are published or not. The documents may come from teaching and research institutions in France or abroad, or from public or private research centers.

L'archive ouverte pluridisciplinaire **HAL**, est destin ee au d ep ot et  a la diffusion de documents scientifiques de niveau recherche, publi es ou non,  emanant des  tablissements d'enseignement et de recherche fran ais ou  trangers, des laboratoires publics ou priv es.

# Development of a Robotic Ultrasound System to Assist Ultrasound Examination of Pregnant Women

Maria Bamaarouf<sup>1</sup>, Flavien Paccot<sup>1</sup>, Laurent Sarry<sup>1</sup>, H el ene Chanal<sup>1</sup>

<sup>1</sup>*Universit e Clermont Auvergne, Clermont Auvergne INP, CNRS, Institut Pascal, F-63000 Clermont-Ferrand*

**Abstract**—This research paper centers on addressing a common issue faced by clinicians during ultrasound examinations, namely work-related musculoskeletal disorders (WRMSDs). The implementation of robotic ultrasound has the potential to reduce these disorders using teleoperated assistance, collaborative support, or even autonomous systems. In this study, we introduce a new collaborative assisting system specifically designed for ultrasound examinations involving pregnant, obese patients. The primary objective is to devise a transparent co-manipulation strategy that enables clinicians to maintain their natural gestures during the procedure. The key principle behind this approach is to ensure that the robot functions as a helpful tool without interfering with the examination process. To achieve this, a novel co-manipulation control strategy is developed, which involves the computation of a virtual solid’s path based on the operator’s interaction. This approach presents numerous benefits in comparison to conventional control techniques. It demonstrates improvements in terms of accuracy, diminishes task execution time, facilitates a more intuitive parameter adjustment process, and necessitates less exertion of force by the operator. Consequently, it could potentially serve as a viable solution for addressing the challenges faced by sonographers. Hence, the potential benefit of this new co-manipulation method is demonstrated experimentally by comparison with impedance and active compliance control strategies.

**Index Terms**—Robotic ultrasound, musculoskeletal disorders, collaborative assistance, obstetrical ultrasound, co-manipulation, hand-guidance.

## I. INTRODUCTION

ULTRASOUND (US) examination, also known as sonography, is a medical imaging technique that uses high-frequency sound waves to produce images of the inside of the body. It is commonly used for various diagnostic purposes, including pregnancy monitoring. During pregnancy, ultrasound examinations are performed for several reasons, including confirming the expected date of delivery, detecting multiple pregnancies, assessing fetal growth, and checking for abnormalities such as birth defects, spina bifida (serious medical condition affecting the spine and often causing paralysis), and heart defects [1], [2]. US is generally considered safe, non-invasive, and painless for both the mother and the unborn baby, [3]. They are an integral part of routine prenatal care and are

recommended by the American College of Obstetricians and Gynecologists (ACOG) [2].

According to the World Health Organization (WHO), the number of obesity cases has almost tripled worldwide since 1975. The WHO estimates that 59% of the global population has excess weight, and 23% suffer from obesity [4]. In the context of pregnancy, obese women face significant health challenges, which can impact fetal scanning and increase complication rates for both the mother and the fetus [5]. Therefore, addressing obesity and its impact on pregnancy is crucial for maternal and fetal health. On the other hand, obesity can also affect the quality of ultrasound imaging, making the assessment of fetal abnormalities more challenging. Notably, in Fig 1 case (B), the amniotic cavity is located at 98 mm in an obese pregnant woman, making it very challenging to establish a correct diagnosis. The importance of ultrasound in prenatal care is often discussed, but the perspective of the physicians who perform this procedure is frequently overlooked. To what extent is this practice influenced by the point of view of the medical professionals?

Ultrasound examination is a strongly user-dependent medical imaging modality that requires highly skilled and experienced sonographers to make proper diagnostics. Medical ultrasound exams often oblige holding the transducer in awkward positions, sometimes applying large forces and performing repetitive motions during examinations. The magnitude of these forces can differ, ranging from 9 to 37N [10], depending on the patient’s body mass index (BMI). Clinicians frequently find themselves in uncomfortable positions when manipulating the probe for extended periods, ranging from 5 to 60 minutes per exam [6]. Apart from identifying the required region of interest, thus being continuously focused on the ultrasound station screen, the examiner also needs to adjust multiple imaging parameters on the ultrasound station. This non-ergonomic examination process has been linked to work-related musculoskeletal disorders (WRMSDs) [7], [8].

Several studies highlight an unusually high incidence of WRMSDs among ultrasound physicians [9]. Manual ultrasonography sessions have been associated with work-related musculoskeletal conditions in a significant percentage of sonographers, ranging from 80 to 90.5% [7]. Factors contributing to the development of WRMSDs among sonographers include poor posture, repetitive movements, transducer pressure, and poor grip (Fig. 2).

Manuscript received December 15, 2023; Revised February 08, 2024; Accepted April 04, 2024. This paper was recommended for publication by Editor Paolo Dario upon evaluation of the Associate Editor and Reviewers’ comments.

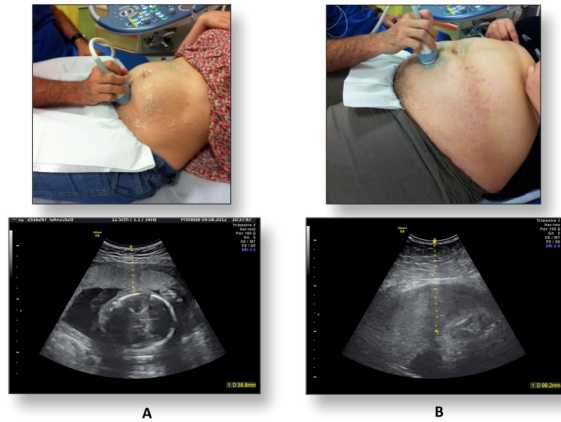


Fig. 1. Example of the impact of obesity on the quality of ultrasound imaging. A: BMI = 25,9; anterior placenta, amniotic cavity at 39 mm. B: BMI = 37, anterior placenta, amniotic cavity at 98 mm. [14]

These conditions include bursitis, muscle strain, and peripheral nerve pathology primarily affecting the upper neck and back region [10], [11]. The impact of these risk factors on the health and well-being of sonographers can lead to pain, sickness absence, surgical procedures, and, in some cases, long-term disability or career-ending injury [7]. Musculoskeletal issues commonly result in disability, causing 67% of sonographers to turn to professional help [11].

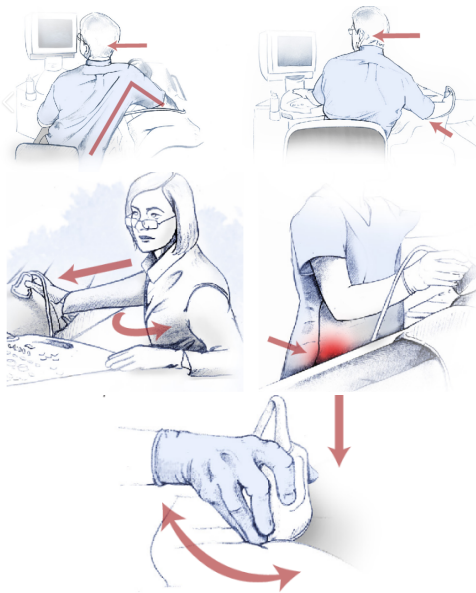


Fig. 2. The main physical risks are related to strength, repetitive motion, awkward postures, and contact pressure. [13]

Scanning pregnant women who are obese continues to present complexities, and at times, it can be a significant issue. According to statistics, more than 80% of sonographers encounter discomfort while conducting scans, and unfortunately, 20% of them eventually experience injuries that lead to the termination of their careers [12].

Nonetheless, robotic ultrasound systems (RUS) has the potential to address the disadvantages associated with traditional ultrasound methods by offering a collaborative assistance,

or even an autonomous system. Assistive robotic ultrasound imaging systems have been developed to provide assistance to sonographers during ultrasonography procedures. This is commonly achieved by minimizing physical strain and enhancing the sonographer's overall comfort. Various types of robots for ultrasound scans have been introduced in the literature [15]. As an illustration, Nakadate et al. [16] introduced a serial robotic system with 3-DoF designed to assist sonographers in supporting their arm to reduce the fatigue during the abdominal diagnosis, while Onogi et al. [17] proposed an US probe manipulator using a parallel link robot with serial 3-DoF links and a 6-axis force sensor, enabling probe manipulation in response to the force exerted by an operator through active compliance control. In parallel Finocchi et al. [18] unveiled a 6-DoF co-robotic ultrasound imaging system that provides force assistance to facilitate US image acquisition through an admittance robot control, while Housden et al. [19] presented a robotic-assisted US image acquisition via a seventeen degrees-of-freedom (17-DoF) dual-probe ultrasound system to enhance the precision of pregnancy scans conducted during the 18-20 week screening. These systems offer various functions, with one specifically tailored to address WRMSDs by utilizing an exoskeleton that requires the clinician to hold the probe, which may not be ideal in obstetrics. On the other hand, autonomous robots present solutions to enhance image acquisition and improve accuracy in diagnostic procedures. Additionally, these systems may not be as adaptable to the diverse morphologies of patients. This article presents an innovative approach designed to alleviate or prevent WRMSDs among medical practitioners. Our concept involves proposing a transparent co-manipulation strategy to ensure that physicians can maintain their natural movements while ensuring that the robot does not disrupt the examination process. The term transparent is employed to signify that the gestures of sonographers remain uninfluenced by the robot. The primary motivation of this research is to assist physicians in addressing a common issue encountered during daily ultrasound scanning, specifically in the examination of pregnant obese patients. This concern was raised by physicians in Clermont-Ferrand, France, and is acknowledged as a prevalent issue among sonographers, as indicated in the literature. Given that physicians are not experts in robotics and their movements are unique and require specific training, it is crucial to prioritize the development of a transparent co-manipulation system. This is essential in order to ensure that our solution is acceptable to them. In this article, we introduce our approach and focus on the initial step of working with the assistive robot, which involves manipulating the robot without influencing the sonographer's usual movements.

In this study, we are using a *Stäubli* robotic arm-the TX2-60. This range of industrial collaborative robots achieves an optimal blend of speed, rigidity, compactness, and precision. With their distinctive features, such as SIL3-PLe safety functions [20], these robots prove versatile across various industries, including sensitive environments. Their safety system complies with integrity standards, ensuring a safe stopping distance, secure speed, tool position limitations, and a safe restart. This robot has been used in different medical scenarios

before. For instance, proposing an innovative solution for interventional oncology robotics [21] and microsurgery [22]. Moreover, an external force/torque sensor is fixed to the robot's end-effector, measuring the operator's applied force during the co-manipulation task. Additionally, the sensor measures the contact force between the probe and the patient's skin. It goes on to explain that these external forces are translated into robot motion. Trajectory generation meticulously controls speed and acceleration thresholds based on the operator's specifications, ensuring a secure working environment. The robot's trajectory is computed by applying Newton's second law to a virtual solid — the transducer. Certainly, the movement of the robot must be regulated through the utilization of mechanical principles that govern the behavior of all solid objects in the physical world. This methodology aims to facilitate the development of a transparent and predictable conduct for the robot. Throughout the examination, the ultrasound probe is co-manipulated by both, the clinician and the robot at different stages (Fig. 3).

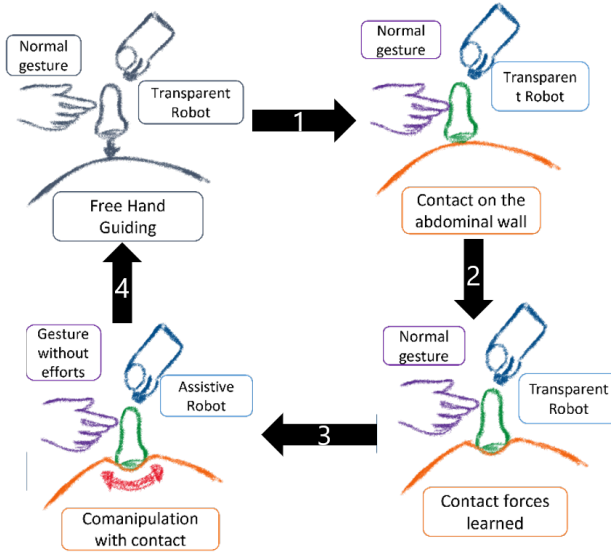


Fig. 3. Different stages of the assisted examination.

- 1) Manual guidance to position the transducer on the patient's abdominal wall.
- 2) Assisted hand guidance with the learning of the contact force imposed by the clinician.
- 3) Co-manipulation of the probe with small displacements while the contact force is held by the robot.
- 4) Assistive hand guiding for the transducer retraction. The co-manipulation should be transparent enough to ensure skill gesture preservation.

To help reduce WRMSDs through our robotic arm, the sonographer will need to bring the robot arm into contact. Once contact is established, the clinician will be hands-free from the probe, as the robot will maintain contact. This, in turn, addresses issues such as transducer pressure, poor grip, and poor posture. We advocate for the use of robotic assistance in prenatal ultrasounds, recognizing the personalized nature of this experience. While maintaining the reassuring presence of

a sonographer, our aim is to safeguard and enhance the interaction between expectant mothers and medical professionals.

In this article, our focus will be directed towards the initial stage of our co-manipulation process, specifically the hand-guidance of the robot to position the transducer on the patient's body. This involves exploring impedance, active compliance, and virtual solid control strategies. The structure of the paper is as follows: it begins with an introduction that outlines the research problem. The second section provides a detailed description of the material and methods employed in this study. The third section presents the findings obtained from the research, while the fourth section engages in a comprehensive discussion of these results. Lastly, the paper concludes with a final section that summarizes the key findings and offers a conclusive statement.

## II. MATERIALS AND METHODS

This application uses a 6-axis industrial collaborative robot. The *Stäubli TX2-60* is an industrial collaborative robot equipped with SIL3-PLe safety functions, facilitating human-machine collaboration [20]. For our medical application the robot is equipped with a 6-axis external force/torque Schunk FTN GAMMA 65-5 sensor and an ergonomic handle-the probe (Fig. 4).

In this section, we'll delve into the reasoning behind our choice to integrate the trajectory calculation system, and we'll introduce our exploration of various control laws. We aim to provide insights into its significance as well as mention different types of control laws in detail such as active compliance and impedance control.

### A. Active compliance control

Within academic literature, one of the strategies employed in human-robot collaboration is a reactive control technique known as "active compliance". This approach, as detailed in [25], empowers collaborative robots with the capability to proactively prevent collisions and injuries during interactions with humans. By implementing active compliance control, the robots acquire the essential flexibility and adaptability required for the skillful accomplishment of complex tasks. In the context of medical applications, active compliance was utilized to facilitate the involvement of a robot in assisting surgeons during knee surgery resections [26]. The employment of compliance ensures that robots can effectively manage uncertainties associated with the position, velocity, size, and shape of the workpiece, thereby reducing the impact of errors [27]. The key factors in active compliance encompass the stiffness and damping coefficients, which are extensively discussed in [28]. The displacement  $(\mathbf{x} - \mathbf{x}_d)$  from the desired position  $\mathbf{x}_d$  is determined based on the applied external forces  $\mathbf{F}_{\text{ext}}$ .

$$\mathbf{M}(\ddot{\mathbf{x}} - \ddot{\mathbf{x}}_d) + \mathbf{C}(\dot{\mathbf{x}} - \dot{\mathbf{x}}_d) + \mathbf{K}(\mathbf{x} - \mathbf{x}_d) = \mathbf{F}_{\text{ext}}, \quad (1)$$

with  $\mathbf{M}$ ,  $\mathbf{C}$  and  $\mathbf{K}$  standing for inertial, damping and stiffness matrices respectively.

Hence, one of the inherent limitations linked to active compliance control lies in scenarios where low stiffness is

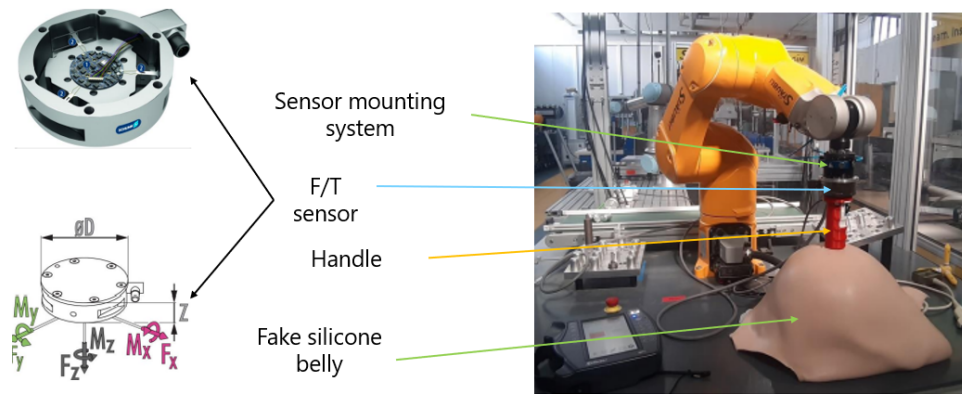


Fig. 4. Experimental set-up: (a) 6-axis external force/torque Schunk FTN GAMMA 65-5 sensor. (b) *Stäubli* TX2-60 and the fake silicone belly.

needed. In such cases, the system's sensitivity to small disturbances becomes a significant issue, as these disturbances can cause unintended deviations from the desired reference paths. This susceptibility can potentially pose safety hazards in the operational setting, emphasizing the crucial aspect that requires meticulous attention during the development and execution of active compliance strategies [29]. Furthermore, the utilization of a stiffness coefficient that enforces effort regardless of the motion negatively impacts the transparency of co-manipulation.

### B. Impedance control

In the literature, impedance control strategy is usually used to regulate the interaction between a robot and its environment, particularly when the robot interacts with external forces or objects. For instance, Suligoj et al. [23] employed impedance control for probe-to-surface contact with the aim of enhancing autonomous ultrasound acquisition and increasing the diagnostic confidence of clinicians. The study introduced a novel integrated medical imaging solution, combining 3D US volume reconstruction and image analysis with autonomous path planning and robot control. Similarly, Von Haxthausen et al. [24] utilized impedance control, incorporating a hierarchical image analysis pipeline that employs convolutional neural networks (CNNs) to control the robot and overcome the limitations of scanning peripheral arteries. Both articles utilized impedance control, complemented by visual servoing, to effectively control the robot autonomously. Impedance is a dynamic control approach that considers both force and speed, allowing the robot to modulate its motion on force perceptions. The impedance makes it possible to define the mechanical behavior of the robotic arm following the formula:

$$\mathbf{M}(\ddot{\mathbf{x}}) + \mathbf{C}(\dot{\mathbf{x}}) = \mathbf{F}_{\text{ext}}, \quad (2)$$

where  $\mathbf{M}$  and  $\mathbf{C}$  represents the inertial and damping matrix respectively, and  $\mathbf{F}_{\text{ext}}$  is the external force vector. This control strategy is particularly useful in applications where robots need to interact with unstructured environments, avoid large impact forces, or work alongside humans. The challenges associated with impedance control in a hand-guiding task encompass the intricate tuning process, as achieving the desired behavior necessitates meticulous tuning of control parameters, a task

that is complex, time-consuming, and depend on the operator. Furthermore, the performance of impedance control in real-world scenarios may be compromised due to the presence of uncertainties in both the robot's control model and the surrounding environment. This sensitivity to uncertainties can result in sub-optimal outcomes. The aforementioned limitations underscore the difficulties that arise when implementing impedance control in robotics, specifically in regards to calibration, vulnerability to uncertainties, and the intricacy of attaining optimal functionality across different operational modes and environments. Additionally, in contrast to the control approach elucidated in the subsequent subsections that governs the position of the robot's end-effector, this particular approach relies on regulating speed.

### C. Virtual Solid

To promote greater transparency within our collaborative system, we present a novel strategy aimed at enhancing usability and effectiveness through an innovative approach to probe co-manipulation. Our proposal involves the creation of a manual control mode, allowing users to effortlessly manipulate the probe by mimicking the natural handling of a regular transducer. This is made possible by incorporating a force sensor that accurately measures external forces exerted by the user, enabling our program to instantaneously translate these forces into real-time robot motion.

In order to ensure an intuitive probe handling, the robot's trajectory should emulate that of a solid in space subjected to forces and/or torques. The computation of the robot's trajectory involves the application of Newton's second law to a virtual solid (Fig. 5). This virtual solid is characterized by a virtual mass  $\mathbf{M}_v$ , virtual inertia matrix  $\mathbf{I}_v$ , and its virtual center of gravity  $G_v$ . The force-screw of external actions  $\mathbf{T}_{\text{ext}}$  applied to the virtual solid is defined by:

$$\{\mathbf{T}_{\text{ext}}\} = \left\{ \begin{array}{l} \mathbf{f}_e + \mathbf{p}_v - \mathbf{f}_{f_v} \\ \mathbf{C}_e + \mathbf{d}_e \times \mathbf{f}_e - \mathbf{C}_{f_v} \end{array} \right\}_{G_v} \quad (3)$$

The operators' applied force is denoted as  $\mathbf{f}_e$ , while the virtual friction force is represented by  $\mathbf{f}_{f_v}$ . The virtual solid weight is given by  $\mathbf{p}_v$ , and the operators' and virtual friction torques are denoted as  $\mathbf{C}_e$  and  $\mathbf{C}_{f_v}$  respectively. The coordinate vector of point  $O_e$  relative to point  $G_v$  is represented by  $\mathbf{d}_e$ .

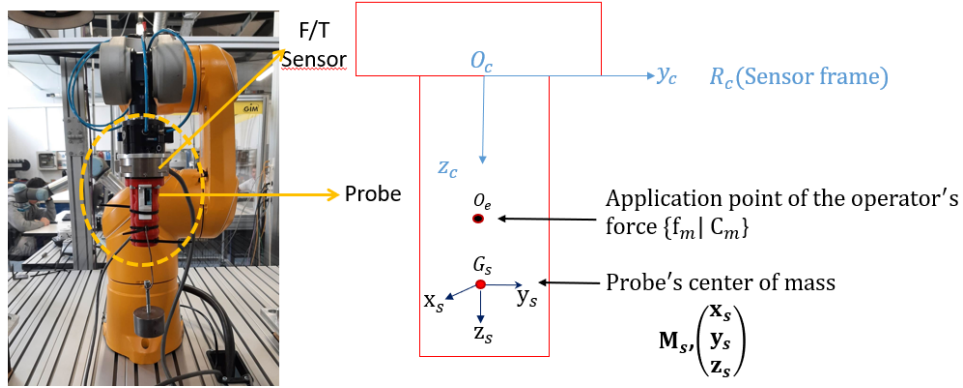


Fig. 5. Virtual solid parameters for the co-manipulation of robotic system.

The *Virtual Solid* method operates on the principle of converting the forces exerted by the operator into the corresponding motion of the robot. Therefore, prior to calculating the tool path, it is necessary to derive the forces applied by the operator based on the measurements obtained from the force sensor. These measured forces are denoted as  $\mathbf{T}_m$  and can be mathematically represented as:

$$\{\mathbf{T}_m\} = \left\{ \mathbf{f}_m \right\}_{O_c} = \left\{ \mathbf{C}_e + \mathbf{d}_s \times \mathbf{p}_s + \mathbf{d}_m \times \mathbf{f}_e \right\}_{O_c} \quad (4)$$

In its frame  $\mathcal{R}_c$ , the force sensor measures the external force/torque as  $\mathbf{f}_m$  and  $\mathbf{C}_m$ . The real weight of the probe is denoted as  $\mathbf{p}_s$ , while  $\mathbf{d}_s$  represents the coordinate vector of point  $G_s$ , which is the mass center of the probe, relative to the origin  $O_c$ . Additionally,  $\mathbf{d}_m$  represents the coordinate vector of point  $O_e$  relative to the origin  $O_c$ . Hence, by determining the probe's weight and the location of its mass center, one can accurately calculate the force exerted by the operator. The robot's motion is then deduced from the Newton's second law applied to a virtual solid through a discrete dual integration. Applying the fundamental principle of dynamics allows us to obtain the desired acceleration ( $\dot{\mathbf{v}}_d, \dot{\boldsymbol{\Omega}}_d$ ) for point  $G_v$ . On account of our specific context, we are considering  $G_v$  and  $O_e$  to be identical and  $\mathbf{p}_v$  is null. Consequently, the acceleration at the point of human-tool interaction can be defined as follows:

$$\begin{cases} \dot{\mathbf{v}}_d = \mathbf{M}_v^{-1}(\mathbf{f}_e - \mathbf{f}_{fv}) \\ \dot{\boldsymbol{\Omega}}_d = \mathbf{I}_v^{-1}(\mathbf{C}_e - \mathbf{C}_{fv}) \end{cases} \quad (5)$$

The friction force and torque, denoted as  $\mathbf{f}_{fv}$  and  $\mathbf{C}_{fv}$  respectively, are calculated based on diagonal matrices that represent the dry and viscous friction coefficients in translation  $\mathbf{F}_{f_{sv}}$  and  $\mathbf{F}_{v_{vv}}$  (eq. (6)).  $\mathbf{C}_{sv}$  and  $\mathbf{C}_{vv}$  represent the coefficients of dry and viscous friction in rotation, respectively (eq. (6)).

$$\begin{cases} \mathbf{f}_{fv} = \mathbf{F}_{f_{sv}} \text{sign}(\mathbf{v}) + \mathbf{F}_{v_{vv}} \mathbf{v} \\ \mathbf{C}_{fv} = \mathbf{C}_{sv} \text{sign}(\boldsymbol{\Omega}) + \mathbf{C}_{vv} \boldsymbol{\Omega} \end{cases} \quad (6)$$

Where  $\mathbf{v}$  is the speed of point  $O_e$  and  $\boldsymbol{\Omega}$  the rotational speed of the probe. These values are estimated from the robot's output.

#### D. Implementation

The control strategy is implemented on CS9 controller in VAL3 language. It is a robotic environment for the construc-

tion of sophisticated and customized applications for *Stäubli* robot. Enhancements have been made to the architecture of the application (Fig. 6), which now contain various tasks such as static sensor calibration, parameter tuning, and addresses security considerations. The hand-guiding application's main features include in-house developed libraries for reading and filtering external forces, as well as performing operator force calculations with safety thresholds and limits. Moreover, it facilitates the choice of different trajectory generation strategies through active compliance, impedance, and virtual solid, depending on the user's preference. The paramount importance of safety is emphasized through continuous monitoring, ensuring a secure working environment at all times. The Table I provides the configuration details for the three examined control strategies parameters. The tuning aims at having similar control behavior in terms of vibrations and operator feedback for each control strategies. We opt for uniform behavior across all directions of the robot axis. Consequently, the values presented in the Table I represent the diagonal elements of the inertia, damping, stiffness matrices and frictions vectors. These terms are denoted as  $m$  for the matrix  $\mathbf{M}$  as an example, and we maintain this formalism for all matrices and vectors. It is important to highlight that, in our experimental setup, the orientation of the end-effector remains constant, with only translation being permitted and calculated.

TABLE I  
CONTROL STRATEGIES SETTINGS.

Control strategies	parameters
Active Compliance	$m = 0.0162kg$ $c = 0.5093Ns/m$ $k = 4N/m$
Impedance	$m = 0.01kg$ $c = 0.02Ns/m$
Virtual Solid (Translation)	$m_v = 4kg$ $f_{sv} = 0.75N$ $f_{vv} = 3Ns/m$

### III. RESULTS

The implementation of the three presented strategies made it possible to compare their behavior experimentally. To assess the effectiveness of different control strategies, we conducted an analysis by replicating the action of relocating the probe

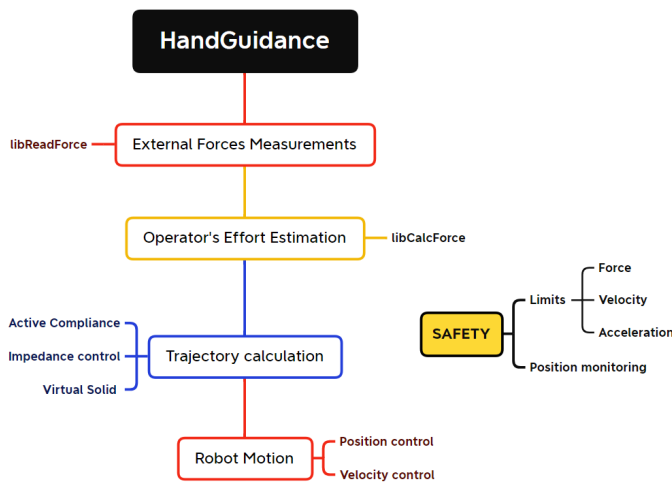


Fig. 6. Hand-Guidance application architecture.

from one location to another on the abdominal surface. This initial step holds significant importance for sonographers. In response to our physician's request, a crucial consideration is the ease of manipulating the robot, akin to handling a 500g probe. The experimental comparison between the virtual solid method and active compliance control, as well as impedance control, reveals notable differences in terms of parameter tuning, the forces required from the operator and, the executed trajectories. In Figure 7 (a), the representation of a XYZ trajectory and a YZ plane trajectory illustrates the paths generated by the three control strategies. We observe that active compliance generates significant vibrations during the movement and lacks stability upon reaching the target points. Impedance control, exhibits a smoother trajectory compared to active compliance, with no vibrations and jerk motion. However, it reveals weaknesses in terms of stability and accuracy when maintaining a fixed position, rendering it unsuitable for ultrasound image acquisition. Concerning the virtual solid method, the experimental findings indicate that parameter tuning is more intuitive, the forces needed for comparable movements are lower in the case of free hand-guidance and the executed trajectory is more in line with the task. Similarly, in Figure 8 (b), we examine the movement executed for each control strategy along with the corresponding time duration for completing the same motion. Active compliance exhibits vibrations and requires approximately five minutes to accomplish the task. In contrast, impedance control takes two minutes, generating less vibration. The virtual solid, meanwhile, completes the task in just a minute and a half, while generating very low vibration. The virtual solid when maintaining position on the targeted points was very accurate compared to the impedance that showed less precision as well as active compliance. Based on the results presented in Table II, we can conclusively have an idea of the ability of a strategy to reach a target repetitively. The X-axis trajectory was chosen to assess the trajectories, as it should have as few variations as possible.

The virtual solid displayed the highest level of precision for the X-axis motion, measuring 381.6 mm compared to

TABLE II  
REPEATABILITY ON THE X-AXIS

Control strategies	Average	Standard dev.	Task duration
Active Compliance	376.359 mm	7.8525 mm	4.6 min
Impedance	370.717 mm	7.0448 mm	2 min
Virtual Solid	381.591 mm	4.5101 mm	1.5 min

the target of 400 mm, with a standard deviation of 4.5 mm. Conversely, both Impedance and active compliance demonstrated similar levels of variability, with standard deviations of 7.04 mm and 7.85 mm, respectively. These findings provide compelling evidence that employing these techniques may result in reduced accuracy when acquiring ultrasound images. In Figure 8(a), the evolution of force in XYZ-axis is observed to vary during the generation of trajectories. It is crucial to emphasize that our operations are carried out with manual guidance, incorporating a constraint of a maximum effort (Restrained Effort in fig. 8) of 1 N to ensure the safety of the working environment. The efforts exerted using the active compliance fluctuate within the range of [-100; 100] Newtons, while impedance and virtual solid exhibit variations around [-50; 50N] and [-10; 10N], respectively. On the other hand, virtual solid demands a reduced amount of force, globally less than 10N fig. 7, aligning with its smooth trajectory. In 8(b), the virtual solid had the best performance as it fluctuated around the control efforts on y and z-axis, but we had almost curves that overlap on the x-axis, proving that forces needed to move the robot are less significant than those needed in impedance control and active compliance scenarios. Importantly, trials have demonstrated that active compliance and impedance control affect our perception of movement. The operator is compelled to exert greater effort to move the robot due to the influence of reactive control on our brain. Conversely, using virtual solid allows freedom of movement of the probe throughout the entire working space without the need for applying large forces.

#### IV. DISCUSSION

Several research studies in the literature have concentrated on improving tele-ultrasound and autonomous robots, contrasting with co-manipulation in obstetrics. Teleoperation involves robots being developed to address the decreasing availability of sonographers. However, teleoperation encounters challenges when dealing with pregnant obese women who may require forces up to 37N during the scan. On the other hand, autonomous robots are primarily utilized to tackle image acquisition issues, which can be difficult in cases involving a pregnant obese woman whose baby is in motion. This approach requires patient acceptance of being diagnosed with a robot. Furthermore, there is a necessity for a robot that enables smooth movement, addressing concerns like transducer pressure, inadequate grip, and improper posture. This calls for a robot that is not entirely autonomous but rather includes the physician in the process, acknowledging the personalized aspect of this medical procedure. This article introduces an innovative approach specifically designed to reduce and even prevent WRMSDs among physicians. The

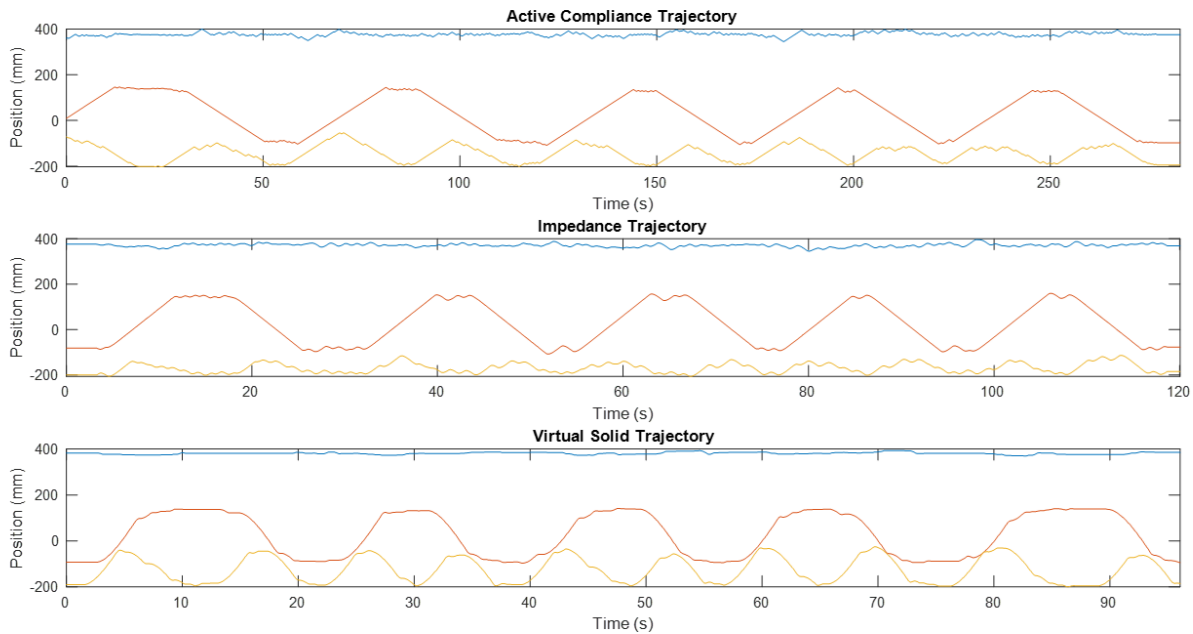
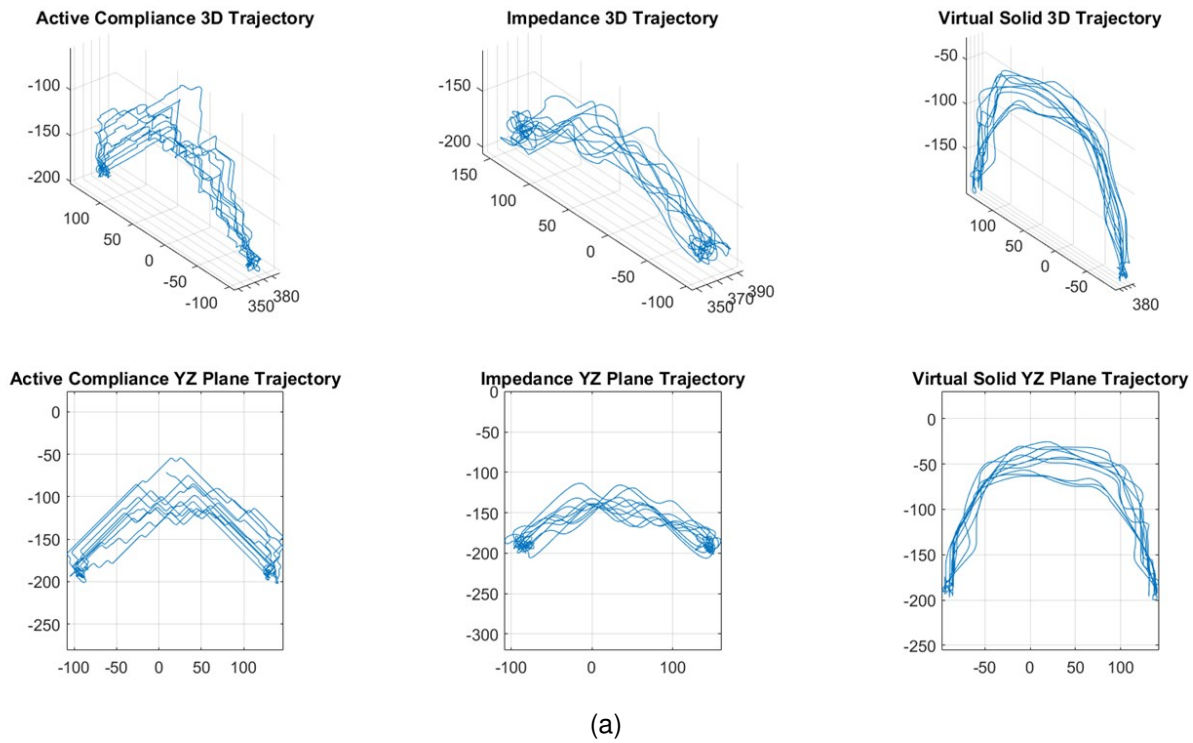
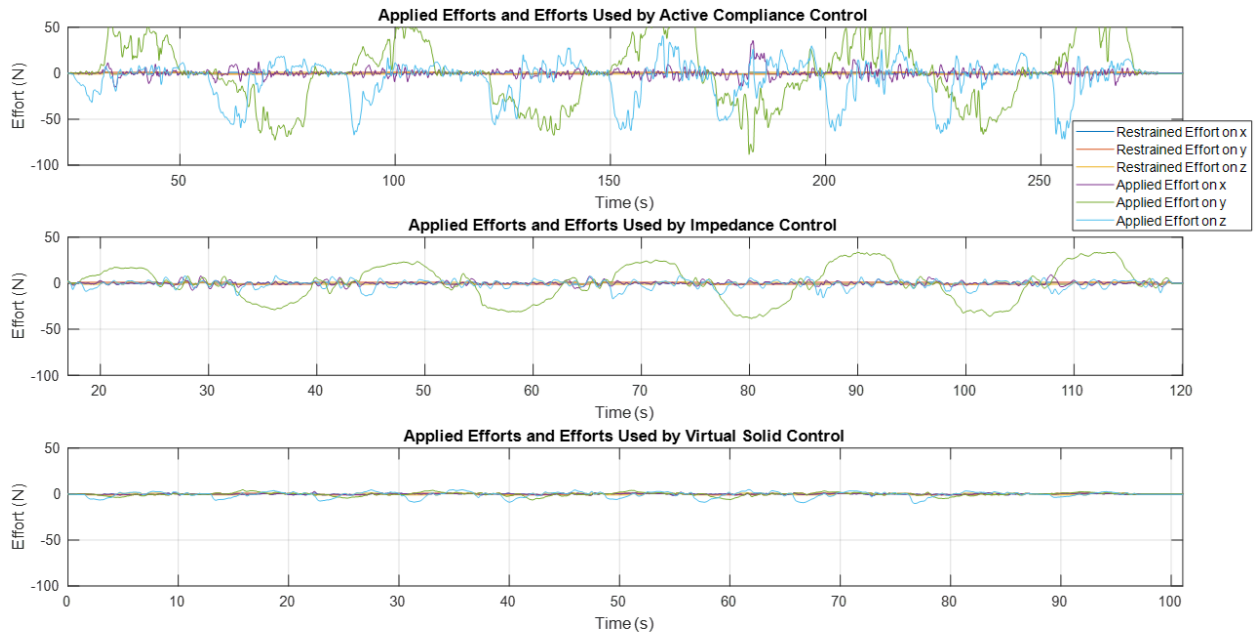


Fig. 7. Comparison of the trajectory of a virtual solid versus the active compliance and the impedance control for a back-and-forth translational motion. In figures (a), the reactive trajectory is represented. The advancement of the tool's Cartesian position along the X-axis regarding time is examined in case (b).

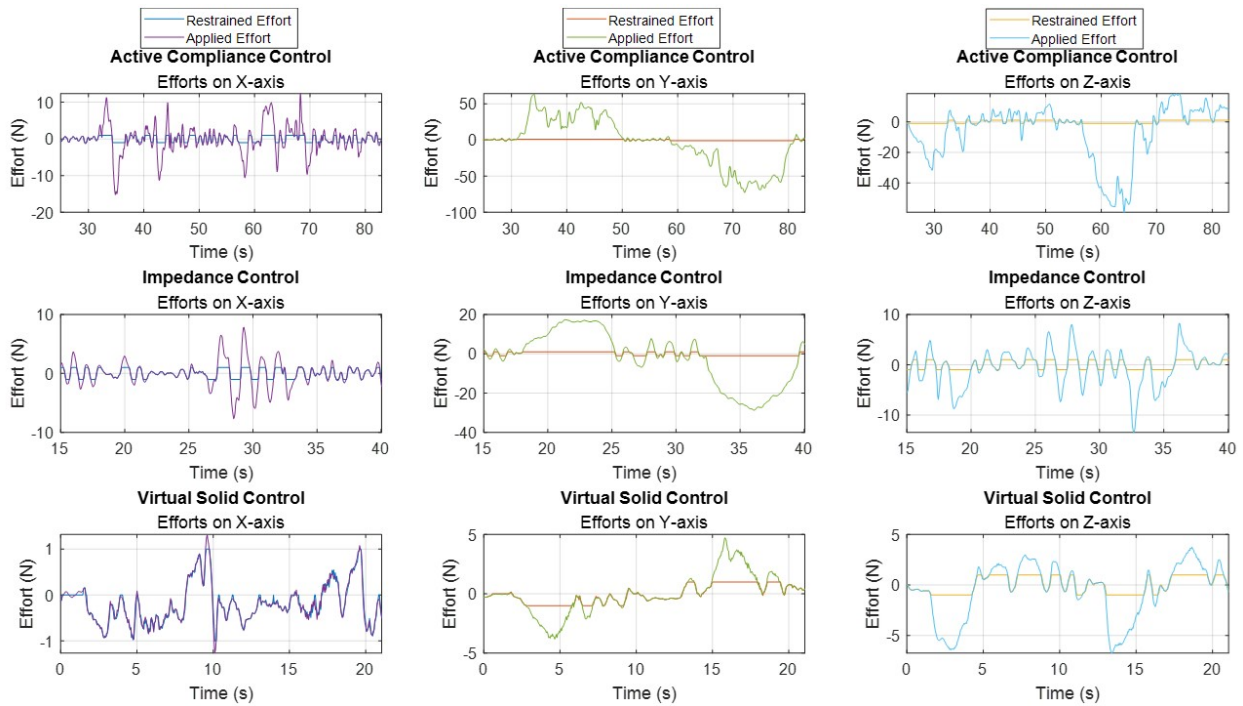
selection of the *Stäubli* TX2-60 for this study, was driven by the robot's high sensitivity and robust safety features. However, an industrial collaborative robot like the *Stäubli* or a collaborative robot such as Kuka or UR5, for example could be considered, as our primary focus in the study is to enhance the WRMSDs among sonographers through

the utilization of mechanical components. Our exploration of control strategies uncovered insights into the challenges associated with impedance control—a dynamic, velocity-based approach. Tuning complexities, sensitivity to uncertainties, and concerns about preventing musculoskeletal disorders in patient interaction make impedance control unsuitable for





(a)



(b)

Fig. 8. Evaluation of efforts between a virtual solid, active compliance, and impedance control for a translational motion is presented. In Figure (a), the applied efforts are illustrated along with the control efforts. A detailed analysis of the efforts generated and constrained during a single movement along the X, Y and Z-axis over time is examined in case (b).

such application. In our pursuit of optimal parameters for damping ( $C$ ) and inertia ( $M$ ), aimed at reducing vibrations in impedance control, we observed a trade-off. While effectively eliminating vibrations, this approach comes at the cost of diminished movement accuracy, resulting in a less transparent co-manipulation experience. This is in contrast with the

smoother trajectory noticed in the virtual solid case, indicating a more continuous and jerk-free motion. The minor perturbations in the virtual solid scenario reflect slight variations in the efforts exerted by the operator. These small variations do not disrupt the movement. While active compliance control offers advantages by modeling the system as a mass-spring-

damper and providing the ability to adjust stiffness, damping, and general impedance, it also presents limitations related to the complexity of parameter tuning. On the other hand, active compliance, a form of position control, allows rapid and unrestricted modification of properties and dynamic behavior but it is vulnerable in low-stiffness scenarios. Experimental findings indicated that relocating the robot-affixed transducer caused sudden, jarring motion sensations and vibrations, potentially causing in real-life scenarios discomfort for both sonographer and patient. Impedance control demonstrates its ability to offer smooth motion but at the expense of reduced accuracy. These considerations should be carefully weighed when choosing between velocity control and position control for a given robotic application, particularly in contexts such as ultrasound examinations. It is worth noting that significant forces exceeding 80N are applied for a simple translation task in the y-axis when utilizing an active compliance control. This presents a challenge in moving the probe as it necessitates greater forces than needed, prolonged execution time, and therefore does not contribute to the reduction of WRMSDs. In contrast, impedance control, which ranges around 30N with no vibrations, demands less force compared to active compliance but these forces are always greater than needed. These distinctions highlight why controlling a robot through impedance control or active compliance results in non-intuitive behavior, requiring continuous reactive effort and potentially leading to musculoskeletal issues. In summary, referring to equation (5), it is proved that the parameters associated with the virtual solid differ from those of active compliance and impedance control. Our experiments demonstrate that Virtual Solid approach enhances usability by enabling a more natural probe manipulation. Namely, the virtual solid stands out for its unique ability to handle both translational and rotational components, represented by vectors indicating linear and angular motions, respectively. In contrast to impedance control and active compliance, which primarily focus on translational aspects, the virtual solid excels in its capacity to address both dimensions of robotic motion as well as addressing WRMSDs issues.

## V. CONCLUSION

In this article, a novel approach to co-manipulation control is introduced, which relies on the calculation of a virtual solid's trajectory during the operator's interaction. Through a comparison with traditional impedance control and active compliance methods, it has been demonstrated that this strategy offers several advantages. Firstly, it facilitates parameter adjustment, making the control process more manageable. Additionally, it reduces the amount of force exerted by the operator, thereby addressing a common issue faced by sonographers. To summarize, this research highlights the significance of careful consideration when choosing and implementing control strategies, with a focus on maintaining a balance between safety, precision, and adaptability. The integration of the Virtual Solid method improves user-friendliness by allowing natural manipulation of the probe and ensuring transparent movement. The project is currently progressing towards the next phase,

which involves co-manipulation in contact with the abdominal wall, but further experiments are required. Once this milestone is achieved, the intention is to utilize ultrasound images for enhanced diagnosis through visual servoing. The ultimate goal of this advancement is to practically incorporate the virtual solid control strategy into real-world medical applications, thereby making a substantial contribution to the ongoing development of human-robot collaboration in healthcare.

## ACKNOWLEDGMENTS

The Ph.D. grant of the primary author of this study was made possible through the generous funding provided by the Université Clermont Auvergne. Additionally, we express our gratitude to the CRI program of CAP2025 and the Hub Innovergne for their financial support in acquiring the force sensor, which played a crucial role in the experimental phase of this research. Furthermore, we extend our thanks to Houssam Eddine Rahem for his valuable contribution to the practical implementation of this study.

## REFERENCES

- [1] *Ultrasound In Pregnancy: What To Expect, Purpose Results*, Cleveland Clinic. Accessed: Nov. 25, 2023. [Online]. Available: <https://my.clevelandclinic.org/health/diagnostics/9704-ultrasound-in-pregnancy>
- [2] *Prenatal Test: Ultrasound (for Parents) - Nemours KidsHealth*. Accessed: Nov. 25, 2023. [Online]. Available: <https://kidshealth.org/en/parents/prenatal-ultrasound.html>
- [3] D. of H. H. Services, *Pregnancy tests - ultrasound*. Accessed: Nov. 25, 2023. [Online]. Available: <http://www.betterhealth.vic.gov.au/health/healthyliving/pregnancy-tests-ultrasound>
- [4] G. Cara, *Obesity and Overweight: Almost One in Two French People Affected. Current Situation, Prevention and Therapeutic Solutions.* Inserm Newsroom. Accessed: Nov. 25, 2023. [Online]. Available: <https://presse.inserm.fr/en/obesite-et-surpoids-pres-dun-francais-sur-deux-concerne-etat-des-lieux-prevention-et-solutions-therapeutiques/66621/>
- [5] V. Mumford and A. Khalil, *Chapter 7 - Ultrasound scanning in early pregnancy and fetal abnormality screening in obese women. in Obesity and Obstetrics (Second Edition)*, T. A. Mahmood, S. Arulkumaran, and F. A. Chervenak, Eds., Elsevier, 2020, pp. 61–68. doi: 10.1016/B978-0-12-817921-5.00007-2.
- [6] *RISK MANAGEMENT OF MUSCULOSKELETAL DISORDERS IN SONOGRAPHY WORK*. Accessed: Aug. 20, 2023. [Online]. Available: <https://1library.net/document/ydo3m31z-risk-management-of-musculoskeletal-disorders-in-sonography-work.html>
- [7] G. Harrison and A. Harris, *Work-related musculoskeletal disorders in ultrasound: Can you reduce risk?* *Ultrasound*, vol. 23, no. 4, pp. 224–230, Nov. 2015, doi: 10.1177/1742271X15593575.
- [8] K. Evans, S. Roll, and J. Baker, *Work-Related Musculoskeletal Disorders (WRMSD) Among Registered Diagnostic Medical Sonographers and Vascular Technologists: A Representative Sample* *Journal of Diagnostic Medical Sonography*, vol. 25, no. 6, pp. 287–299, Nov. 2009, doi: 10.1177/8756479309351748.
- [9] S. E. Salcudean, G. Bell, S. Bachmann, W. H. Zhu, P. Abolmaesumi, and P. D. Lawrence, *Robot-Assisted Diagnostic Ultrasound – Design and Feasibility Experiments in Medical Image Computing and Computer-Assisted Intervention – MICCAI'99*, vol. 1679, C. Taylor and A. Colchester, Eds., in *Lecture Notes in Computer Science*, vol. 1679, Berlin, Heidelberg: Springer Berlin Heidelberg, 1999, pp. 1062–1071. doi: 10.1007/10704282115.
- [10] M. Muir, P. Hrynkow, R. Chase, D. Boyce, and D. Mclean, “The nature, cause, and extent of occupational musculoskeletal injuries among sonographers: Recommendations for treatment and prevention,” *J. Diagn. Med. Sonography*, vol. 20, no. 5, pp. 317–325, 2004.
- [11] Roshan, Mariadas Capsran, Adrian Pranata, and Mats Isaksson. “Robotic Ultrasonography for Autonomous Non-Invasive Diagnosis—A Systematic Literature Review.” *IEEE Transactions on Medical Robotics and Bionics* (2022).

- [12] C. Ulrich and L. N. S. Andreasen Struijk, *Probe contact forces during obstetric ultrasound scans - A design parameter for robot-assisted ultrasound*, International Journal of Industrial Ergonomics, vol. 86, p. 103224, Nov. 2021, doi: 10.1016/j.ergon.2021.103224.
- [13] S. Murphey, "Work Related Musculoskeletal Disorders in Sonography," Journal of Diagnostic Medical Sonography, vol. 33, no. 5, pp. 354–369, Sep. 2017, doi: 10.1177/8756479317726767.
- [14] D. Lemery, B. Chauveau, A. Legrand, and L. Boyer, *L'échographie obstétricale chez la femme obèse*. Revue de Médecine Périnatale, vol. 8, no. 4, pp. 180–186, 2016, doi: 10.1007/s12611-016-0389-1.
- [15] von Haxthausen F, Böttger S, Wulff D, Hagenah J, García-Vázquez V, Ipsen S. Medical Robotics for Ultrasound Imaging: Current Systems and Future Trends. Curr Robot Rep. 2021;2(1):55-71. doi: 10.1007/s43154-020-00037-y. Epub 2021 Feb 22. PMID: 34977593; PMCID: PMC7898497.
- [16] R. Nakadate et al., "Development of robot assisted measurement system for abdominal ultrasound diagnosis," 2010 3rd IEEE RAS EMBS International Conference on Biomedical Robotics and Biomechatronics, Tokyo, Japan, 2010, pp. 367-372, doi: 10.1109/BIOROB.2010.5627716.
- [17] Onogi, Shinya, et al. "Robotic ultrasound probe handling auxiliary by active compliance control." Advanced Robotics 27.7 (2013): 503-512.
- [18] Finocchi, Rodolfo, et al. "Co-robotic ultrasound imaging: A cooperative force control approach." Medical Imaging 2017: Image-Guided Procedures, Robotic Interventions, and Modeling. Vol. 10135. SPIE, 2017.
- [19] Housden, James, et al. "Towards standardized acquisition with a dual-probe ultrasound robot for fetal imaging." IEEE robotics and automation letters 6.2 (2021): 1059-1065.
- [20] <https://www.staubli.com/fr/fr/robotics/produits/robots-industriels/tx2-60.html>
- [21] <https://www.quantumsurgical.com/epione/>
- [22] <https://www.bhs-technologies.com/>
- [23] Suligoj, Filip, et al. "RobUST—an autonomous robotic ultrasound system for medical imaging." IEEE Access 9 (2021): 67456-67465.
- [24] Von Haxthausen, F., Hagenah, J., Kaschwich, M., Kleemann, M., García-Vázquez, V., Ernst, F. (2020, September). Robotized ultrasound imaging of the peripheral arteries—a phantom study. In Current Directions in Biomedical Engineering (Vol. 6, No. 1, p. 20200033). De Gruyter.
- [25] A. D. Santis, B. Siciliano, and N. Federico, *SAFETY ISSUES FOR HUMAN-ROBOT COOPERATION IN MANUFACTURING SYSTEMS*, 2008.
- [26] B. L. Davies, S. J. Harris, W. J. Lin, R. D. Hibberd, R. Middleton, and J. C. Cobb, *Active compliance in robotic surgery—the use of force control as a dynamic constraint*, Proc Inst Mech Eng H, vol. 211, no. 4, pp. 285–292, 1997, doi: 10.1243/0954411971534403.
- [27] P. Petrovic and N. Lukic, *Configuration-based compliance control of kinematically redundant robot arm Part I: Theoretical framework*, FME Transactions, vol. 45, pp. 468–474, Jan. 2017, doi: 10.5937/fmet1704468P.
- [28] J. Huang et al., *A strategy for human-robot collaboration in taking products apart for remanufacture*, FME Transactions, vol. 47, pp. 731–738, Jan. 2019, doi: 10.5937/fmet1904731H.
- [29] A. Scibilia, M. Laghi, E. De Momi, L. Peternel, and A. Ajoudani, *A Self-Adaptive Robot Control Framework for Improved Tracking and Interaction Performances in Low-Stiffness Teleoperation*, in 2018 IEEE-RAS 18th International Conference on Humanoid Robots (Humanoids), Beijing, China: IEEE, Nov. 2018, pp. 280–283. doi: 10.1109/HUMANOIDS.2018.8625062.
- [30] M. Schumacher, J. Wojtusich, P. Beckerle, and O. von Stryk, *An introductory review of active compliant control*, Robotics and Autonomous Systems, vol. 119, pp. 185–200, Sep. 2019, doi: 10.1016/j.robot.2019.06.009.

## VI. BIOGRAPHY SECTION

**Maria Bamaarouf** as a Ph.D. student and the vice-president of Doct'Auvergne (association of Ph.D. students and young researchers in the Auvergne region), earned her master's degree from Sorbonne University in the field of medical engineering. Her specialty lies in mechatronics systems for rehabilitation.

**Flavien Paccot** received the Ph.D. degree in robotics from Université Blaise Pascal in 2009. Since 2008, he has been a teacher at Université d'Auvergne. His research interests include robotics, control, and co-manipulation.

**Laurent Sarry** obtained his Ph.D. in medical image processing in 1996. He subsequently became an associate professor and, since 2006, a full professor at the Ecole Universitaire de Physique et d'Ingénierie. His research interests at the Institut Pascal include computer-assisted diagnosis, patient-specific simulation, and gesture assistance.

**Hélène Chanal** received her Ph.D. degree in mechanical engineering from Université Blaise Pascal in 2006. Since 2007, she has been an associate professor at SIGMA Clermont. Her research interests include the identification and modeling of machine and robot behavior.